



## City Research Online

### City, University of London Institutional Repository

---

**Citation:** Giaralis, A. ORCID: 0000-0002-2952-1171 and Taflanidis, A. A. (2015). Reliability-based design of tuned mass-damper-inerter (TMDI) equipped multi-storey frame buildings under seismic excitation. In: Proceedings of the 12th International Conference on Applications of Statistics and Probability in Civil Engineering (ICASP12). . Vancouver: University of British Columbia Library. ISBN 9780888652454

This is the published version of the paper.

This version of the publication may differ from the final published version.

---

**Permanent repository link:** <https://openaccess.city.ac.uk/id/eprint/19263/>

**Link to published version:** 10.14288/1.0076257

**Copyright:** City Research Online aims to make research outputs of City, University of London available to a wider audience. Copyright and Moral Rights remain with the author(s) and/or copyright holders. URLs from City Research Online may be freely distributed and linked to.

**Reuse:** Copies of full items can be used for personal research or study, educational, or not-for-profit purposes without prior permission or charge. Provided that the authors, title and full bibliographic details are credited, a hyperlink and/or URL is given for the original metadata page and the content is not changed in any way.

---

City Research Online:

<http://openaccess.city.ac.uk/>

[publications@city.ac.uk](mailto:publications@city.ac.uk)

---

# Reliability-based Design of Tuned Mass-Damper-Inerter (TMDI) Equipped Multi-storey Frame Buildings under Seismic Excitation

Agathoklis Giaralis

Senior Lecturer, Dept. of Civil Engineering, City University London, London, UK

Alexandros A. Taflanidis

Associate Professor, Dept. of Civil and Environmental Engineering and Earth Sciences, University of Notre Dame, Notre Dame, IN 46556, USA

**ABSTRACT:** The reliability based optimal design is considered of tuned mass-damper-inerter (TMDI) equipped linear building frames subject to seismic excitations modeled as stationary colored random processes. The TMDI is a recently introduced generalization of the classical linear tuned mass-damper (TMD) benefitting from the mass amplification property, the so-called inertance, of the inerter device to enhance the vibration suppression capabilities of the TMD. The frequency, damping ratio, and inertance TMDI properties are treated as design variables to minimize out-crossing rates of pre-specified thresholds for building floor accelerations, inter-storey drifts, and TMDI mass displacement. Numerical data pertaining to a 10-storey frame structure equipped with a TMDI arranged in 12 different topologies are furnished indicating the enhanced performance of the TMDI over the classical TMD especially for relatively small additional attached mass.

## 1. INTRODUCTION

Over the past several decades, the concept of the tuned mass-damper (TMD) has been extensively considered for the protection of building structures exposed to earthquake hazards in the context of passive vibration control (e.g., Rana and Soong 1998, Hoang et al. 2008). The TMD comprises a mass attached towards the top of the structure whose vibration motion is to be controlled (primary structure) via optimally designed/"tuned" linear spring and dashpot elements. Although closed-form expressions for optimum TMD properties do exist (e.g., Tigli 2012), numerical optimization routines are commonly employed for TMD design. No matter what performance criteria are adopted in this design, it is widely recognized that the TMD effectiveness for the seismic protection of structures depends heavily on its inertia properties (e.g., Hoang et al. 2008, Moutinho 2012). Practically speaking, the larger the attached TMD mass that can be accommodated, subject to structural design and architectural constraints, the more effective the TMD will be.

In this regard, recently, a generalization of the classical TMD has been proposed by Marian and Giaralis (2013 and 2014) incorporating an "inerter" device: the tuned mass-damper-inerter (TMDI). The inerter is a two-terminal mechanical device developing a resisting force proportional to the relative acceleration of its terminals (Smith 2002). The underlying constant of proportionality ("inertance") can be orders of magnitude larger than the physical mass of the device. In this regard, it was shown analytically and numerically that optimally designed TMDI, treating the attached mass and inertance as fixed quantities, outperforms the classical TMD in terms of relative displacement variance of linear primary structures under broad-band and narrow-band stochastic base excitations by exploiting the "mass amplification" property of the inerter (Marian and Giaralis 2014).

This paper investigates the optimal reliability-based design of the TMDI characteristics for seismic applications. Linear damped primary structures are considered base-excited by filtered stationary white noise

representing the seismic input action. Compared to the work by Marian and Giaralis (2013, 2014), this study offers some new insights; it adopts as design objective the optimization of the first-passage probability beyond certain thresholds for building floor accelerations, interstorey drifts, and attached mass displacement (stroke) as opposed to minimizing solely the variance of the top floor displacement; it considers the inertance property as a design parameter, not taken as *a priori* fixed; it examines different TMDI topologies whereas the TMDI mass is attached at intermediate floors within a typical framed structure using different connectivity arrangements, apart from the practically most obvious one: the TMDI mass is attached to the top floor via the spring and the damper and linked to one floor below via the inerter. The governing equations of motion for a structure equipped with a TMDI are reviewed in the next section, followed (Section 3) by a discussion of the first-passage reliability-based design. Section 4 presents a case study for a 10-storey TMDI equipped building frame exposed to stochastic seismic excitation. Concluding remarks and extensions are finally discussed in Section 5.

## 2. THE TUNED MASS-DAMPER-INERTER (TMDI) SYSTEM FOR MULTI-STOREY FRAME BUILDING STRUCTURES

### 2.1. The ideal inerter

Conceptually introduced by Smith (2002), the ideal inerter is a linear two terminal device of negligible mass/weight developing an internal (resisting) force  $F$  proportional to the relative acceleration of its terminals which are free to move independently. Its force is expressed as

$$F = b(\ddot{u}_1 - \ddot{u}_2), \quad (1)$$

where  $u_1$  and  $u_2$  are the displacement coordinates of the inerter terminals as shown in Figure 1 and, hereafter, a dot over a symbol signifies differentiation with respect to time. In the above equation, the constant of proportionality  $b$  is the so-called inertance and has mass units. It fully characterizes the behavior of the ideal inerter.

Importantly, the physical mass of actual inerter devices can be two or more orders of magnitude lower than  $b$ . This has been experimentally validated by testing several flywheel-based prototyped inerter devices incorporating rack-and-pinion or ball-screw mechanisms to transform the translational kinetic energy into rotational kinetic energy “stored” in a relatively light rotating disk (e.g., Papageorgiou and Smith 2004). More recently, hydraulic-based inerters achieving inertance values  $b$  that are almost independent of the physical device mass were also experimentally verified (Wang et al. 2011, Swift et al. 2013). In this regard, the ideal inerter can be construed as an inertial amplification device, since by “grounding” any one of its terminals, the device acts as a “weightless” mass  $b$ . This consideration led to the tuned mass-damper-inerter system, which may enhance the vibration suppression capabilities of the classical tuned mass-damper for the same attached mass (and thus weight) by utilizing the inertial amplification property of the inerter (Marian and Giaralis 2013 and 2014).

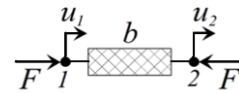


Figure 1: Schematic of an ideal inerter device

### 2.2. Equations of motion of the TMDI system

The topology of the tuned mass-damper-inerter (TMDI) configuration originally proposed by Marian and Giaralis (2013) for planar base-excited  $n$ -storey frame building primary structures modeled as lumped-mass multi-degree-of-freedom (MDOF) “chain-like” linear damped systems is shown in Figure 2. It involves a classical tuned mass-damper (TMD) located at the top floor of the primary structure comprising a mass  $m_d$  attached to the structure via a linear spring of stiffness  $k_d$  and a linear dashpot of damping coefficient  $c_d$ . The TMD mass is linked to the penultimate frame floor by an inerter device with inertance  $b$ . Herein, a significantly more general formulation is adopted allowing for the consideration of different TMDI topologies

in which the TMD is attached to the  $i_d$  floor and is linked via an inerter to the  $i_b$  floor. This generalization is accomplished by means of properly defined *location* and *connectivity* vectors as detailed below.

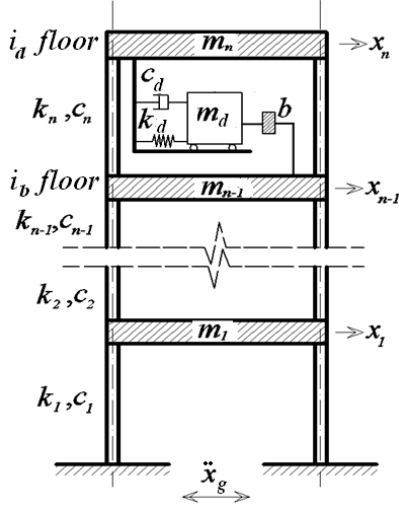


Figure 2: Tuned mass-damper-inerter (TMDI) equipped seismically excited multi-storey frame.

Let  $\mathbf{x}_s \in \mathbb{R}^n$  be the vector collecting the floor displacements of the primary structure relative to the ground motion. Denote by  $\mathbf{R}_d \in \mathbb{R}^n$  the *TMD location* vector specifying the floor the TMD is attached to (i.e., vector of zeros with a single one in its  $i_d$  entry), and by  $\mathbf{R}_b \in \mathbb{R}^n$  be the *inerter location* vector specifying the floor the inerter is connected to (i.e., vector of zeros with a single one in its  $i_b$  entry). Let, also,  $y \in \mathbb{R}$  be the displacement of the TMD mass relative to the  $i_d$  floor and define the *connectivity* vector by  $\mathbf{R}_c = \mathbf{R}_d - \mathbf{R}_b$ . Then, the resisting force  $F$  developing within the inerter is equal to  $b(\mathbf{R}_c \ddot{\mathbf{x}}_s + \dot{y})$ . Further, the coupled equations of motion for the TMDI equipped structure in Figure 2 is

$$\begin{aligned} & (\mathbf{M}_s + \mathbf{R}_d m_d \mathbf{R}_d^T + \mathbf{R}_c b \mathbf{R}_c^T) \ddot{\mathbf{x}}_s + (m_d \mathbf{R}_d + b \mathbf{R}_c) \dot{y} \\ & + \mathbf{C}_s \dot{\mathbf{x}}_s + \mathbf{K}_s \mathbf{x}_s = -(\mathbf{M}_s + \mathbf{R}_d m_d \mathbf{R}_d^T) \mathbf{R}_s \ddot{x}_g \end{aligned} \quad (2)$$

and

$$\begin{aligned} & (m_d + b) \ddot{y} + (m_d \mathbf{R}_d^T + b \mathbf{R}_c^T) \ddot{\mathbf{x}}_s \\ & + c_d \dot{y} + k_d y = -m_d \mathbf{R}_d^T \mathbf{R}_s \ddot{x}_g \end{aligned}, \quad (3)$$

where  $\mathbf{M}_s \in \mathbb{R}^{n \times n}$ ,  $\mathbf{C}_s \in \mathbb{R}^{n \times n}$ , and  $\mathbf{K}_s \in \mathbb{R}^{n \times n}$  are the mass, damping, and stiffness matrices of the primary structure; and  $\mathbf{R}_s \in \mathbb{R}^{n \times 1}$  is the influence vector. Note that in deriving the previous two equations the inerter is taken as weightless, similarly to the spring and to the dashpot, and, therefore, and it does not attract any horizontal seismic inertial force (see also Takewaki et al. 2012, and Marian and Giaralis 2014). Moreover, Eq. (3) suggests that the total inertia of the TMDI is equal to  $(m_d + b)$ . This observation motivates the definition of the following dimensionless frequency ratio  $f_d$ , damping ratio  $\zeta_d$ , inertance ratio  $\beta$ , and mass ratio  $\mu$

$$f_d = \sqrt{\frac{k_d}{(m_d + b)}} / \omega_1; \quad \zeta_d = \frac{c_d}{2(m_d + b)\omega_d} \quad (4)$$

$$\beta = b / M \quad ; \quad \mu = m_d / M$$

to characterize the design of the TMDI (Marian and Giaralis 2015), where  $\omega_1$  and  $M$  is the fundamental natural frequency and the total mass of the primary structure.

### 3. RELIABILITY-BASED DESIGN UNDER STATIONARY EXCITATION

Let  $\ddot{x}_g$  in Eqs. (2) and (3) be a stochastic stationary process modeled as filtered Gaussian white noise. Augmentation of the models for the excitation and for the structure leads to the following state-space system representation

$$\dot{\mathbf{x}}(t) = \mathbf{A}(\boldsymbol{\varphi})\mathbf{x}(t) + \mathbf{E}(\boldsymbol{\varphi})w(t); \quad \mathbf{z}(t) = \mathbf{C}(\boldsymbol{\varphi})\mathbf{x}(t) \quad (5)$$

where  $\mathbf{x}(t) \in \mathbb{R}^{n_x}$  is the state vector;  $\mathbf{z}(t) \in \mathbb{R}^{n_z}$  is the vector of performance variables (response output of the system) with  $z_i$  denoting the  $i^{\text{th}}$  output;  $w(t) \in \mathbb{R}$  is a zero-mean Gaussian white-noise process with spectral intensity equal to one; and  $\mathbf{A}(\boldsymbol{\varphi})$ ,  $\mathbf{E}(\boldsymbol{\varphi})$ ,  $\mathbf{C}(\boldsymbol{\varphi})$  are the state-space matrices that are a function of vector  $\boldsymbol{\varphi}$ , which represents the controllable parameters of the TMDI system ( $\beta$ ,  $f_d$  and  $\zeta_d$ ). Note that the proposed formulation takes into account the spectral characteristics of the stochastic excitation, by appropriate augmentation of the state equation (Taflanidis and Scruggs 2010). This allows for an efficient calculation of the response statistics for the augmented system.

### 3.1. Stationary response statistics

Under the modelling assumptions discussed above, the output of the system,  $\mathbf{z}(t)$ , has a Gaussian distribution with zero mean and covariance matrix in stationary response given as

$$\mathbf{K}_{zz} = \mathbf{C}(\boldsymbol{\varphi})\mathbf{P}(\boldsymbol{\varphi})\mathbf{C}(\boldsymbol{\varphi})^T, \quad (6)$$

where the state covariance matrix,  $\mathbf{P}(\boldsymbol{\varphi})$ , is determined by the solution of the following Lyapunov equation (Lutes and Sarkani 1997)

$$\mathbf{A}(\boldsymbol{\varphi})\mathbf{P}(\boldsymbol{\varphi}) + \mathbf{P}(\boldsymbol{\varphi})\mathbf{A}(\boldsymbol{\varphi})^T + \mathbf{E}(\boldsymbol{\varphi})\mathbf{E}(\boldsymbol{\varphi})^T = 0. \quad (7)$$

For each of system output variables  $z_i$ ,  $i = 1, \dots, n_z$  described as  $z_i = \mathbf{n}_i^T \mathbf{z}$  its variance is

$$\sigma_{z_i}^2 = \mathbf{n}_i^T \mathbf{C}(\boldsymbol{\varphi})\mathbf{P}(\boldsymbol{\varphi})\mathbf{C}(\boldsymbol{\varphi})^T \mathbf{n}_i \quad (8)$$

In evaluating the reliability-based performance, the variance of the derivative of the components of  $\mathbf{z}$  needs to be computed whereas for the problem to be well-posed (i.e., have finite out-crossing rate), the relationship  $\mathbf{C}(\boldsymbol{\varphi})\mathbf{E}(\boldsymbol{\varphi}) = 0$  needs to hold (Taflanidis and Scruggs 2010). Under this assumption, the variance of  $\dot{z}_i$  is

$$\sigma_{\dot{z}_i}^2 = \mathbf{n}_i^T \mathbf{C}(\boldsymbol{\varphi})\mathbf{A}(\boldsymbol{\varphi})\mathbf{P}(\boldsymbol{\varphi})\mathbf{A}(\boldsymbol{\varphi})^T \mathbf{C}(\boldsymbol{\varphi})^T \mathbf{n}_i \quad (9)$$

Further, the transfer function for  $z_i$  is

$$\mathbf{H}_{z_i}(\omega; \boldsymbol{\varphi}) = \mathbf{n}_i^T \mathbf{C}(\boldsymbol{\varphi})[i\omega\mathbf{I} - \mathbf{A}(\boldsymbol{\varphi})]^{-1} \mathbf{E}(\boldsymbol{\varphi}). \quad (10)$$

### 3.2. First passage reliability-based design

Consider an hyper-rectangular domain  $D_s \subset \mathcal{R}^{n_z}$  in the space of the performance variables  $\mathbf{z}(t)$  as

$$D_s = \{\mathbf{z}(t) \in \mathcal{R}^{n_z} : |z_i(t)| < \beta_i, \forall i = 1, \dots, n_z\}, \quad (11)$$

to define the acceptable performance (Figure 3). Region  $D_s$  is bounded by the hyperplane pairs  $B_i$ :  $|z_i| = \beta_i$ ,  $i = 1, \dots, n_z$  and by appropriate definition of the  $\mathbf{z}(t)$  can represent any desired limit state function. The reliability calculation pertains to the estimation of the probability that within some time duration  $T$ , any of the performance variables out-crosses the boundary, written as

$$P_F(\boldsymbol{\varphi} | T) = P[\mathbf{z}(\tau) \notin D_s \text{ for some } \tau \in [0, T]]. \quad (12)$$

If  $S_D$  is the boundary of  $D_s$ , then  $P_F(\boldsymbol{\varphi} | T)$  is expressed as the probability of first passage across  $S_D$ , which in stationary conditions is

$$P_F(\boldsymbol{\varphi} | T) = 1 - \exp(-\nu_z^+(\boldsymbol{\varphi})T), \quad (13)$$

where  $\nu_z^+(\boldsymbol{\varphi})$  is the mean out-crossing rate of the boundary  $S_D$ , conditioned on no previous out-crossing having occurred (Taflanidis and Beck 2006). The reliability-based design corresponds then to identification of the design variables that minimizes the failure probability

$$\boldsymbol{\varphi}^* = \arg \min_{\boldsymbol{\varphi} \in \Phi} [P_F(\boldsymbol{\varphi} | T)] = \arg \min_{\boldsymbol{\varphi} \in \Phi} [\nu_z^+(\boldsymbol{\varphi})], \quad (14)$$

where  $\Phi$  denotes the admissible design space for the design variables. This design problem requires calculation of the out-crossing rate.

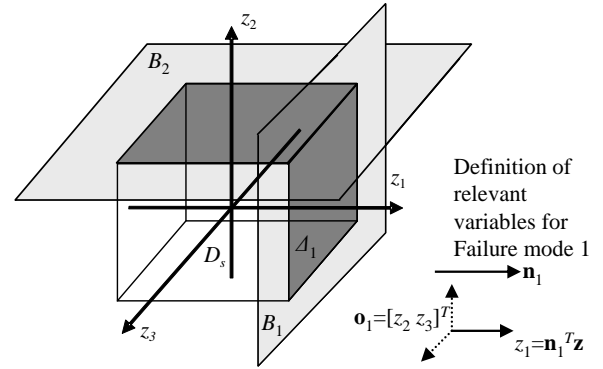


Figure 3: First-passage problem for a three dimensional response output

### 3.3. Out-crossing rate calculation

As shown in Taflanidis and Beck (2006), for vector processes  $\mathbf{z}(t)$ , the out-crossing rate can be accurately approximated by a summation of the individual out-crossing rates over each linear surface of the boundary (corresponding to the failure mode associated  $z_i$ )

$$\nu_z^+(\boldsymbol{\varphi}) \approx \sum_{i=1}^{n_z} P_{z_i}(\boldsymbol{\varphi}) [\lambda_{z_i}(\boldsymbol{\varphi}) r_{z_i}^+(\boldsymbol{\varphi})]. \quad (15)$$

Each of the individual out-crossing rates is a product of three factors: Rice's unconditional out-crossing rate  $r_{z_i}^+(\boldsymbol{\varphi})$ , the temporal-correlation correction factor  $\lambda_{z_i}(\boldsymbol{\varphi})$ , and the spatial-correlation weighting factor  $P_{z_i}(\boldsymbol{\varphi})$ . The product of the first two is the conditional out-crossing rate for scalar  $z_i$  over  $|z_i| = \beta_i$  whereas  $P_{z_i}(\boldsymbol{\varphi})$  facilitates the extension to the vector case and accounts for the correlation between failure events on different surfaces of  $S_D$ .

Considering these different factors, Rice's out-crossing rate is given by (Rice 1944, 1945)

$$r_{z_i}^+(\boldsymbol{\varphi}) = \sigma_{z_i} / (\pi\sigma_{z_i}) \exp\left\{-\beta_i^2 / (2\sigma_{z_i}^2)\right\}, \quad (16)$$

with the required variances given by Eqs. (8) and (9). This rate considers out-crossings over the entirety of the pair of hyperplanes  $B_i$ . Further it assumes independence between out-crossing events for the process  $z_i$ . A temporal correlation factor  $\lambda_{z_i}(\boldsymbol{\varphi})$  may be utilized to approximately address errors introduced by this independence assumption. The correction factor proposed by Taflanidis and Beck (2006) is adopted here for this purpose, given by

$$\lambda_{z_i}(\boldsymbol{\varphi}) \approx \frac{1 - \exp\left\{-q^{0.6} \left(\frac{2}{\sqrt{\pi}}\right)^{0.1} \frac{\beta_i \sqrt{2}}{\sigma_{z_i}}\right\}}{1 - \exp\left(-\beta_i^2 / (2\sigma_{z_i}^2)\right)}, \quad (17)$$

where for a process with spectral density  $S_{z_i z_i}$

$$q = \sigma_{z_i}^6 / (4\pi \int_{-\infty}^{\infty} |\omega| S_{z_i z_i}(\omega) d\omega \int_{-\infty}^{\infty} S_{z_i z_i}^2(\omega) d\omega) \quad (18)$$

and for the calculation of the integrals in the denominator, the spectral density  $S_{z_i z_i}$  is substituted by the equivalent expression  $\mathbf{H}_{z_i}(\omega; \boldsymbol{\varphi}) \mathbf{I} \mathbf{H}_{z_i}(\omega; \boldsymbol{\varphi})^*$  with  $\mathbf{H}_{z_i}(\omega; \boldsymbol{\varphi})$  given by Eq. (10). The frequency range over which the dynamics of system are important is partitioned at desired points and the frequency response is calculated. The one-dimensional integral is then evaluated via standard numerical integration.

Finally,  $P_{z_i}(\boldsymbol{\varphi})$  is evaluated as follows. If  $\Delta_i$  is the hyper-polygon (dark shaded area in Figure 3) corresponding to the intersection of  $S_D$  and of any of the pair of hyper-planes  $B_i$ , and  $\mathbf{o}_i$  is the orthogonal component of  $\mathbf{z}$ , then  $P_{z_i}(\boldsymbol{\varphi})$  corresponds to the probability that  $\mathbf{o}_i \in \Delta_i$  when the out-crossing event occurs for  $z_i$ ,

$$P_{z_i}(\boldsymbol{\varphi}) = P[\mathbf{o}_i \in \Delta_i | z_i = \beta_i]. \quad (19)$$

This ultimately constitutes a  $(n_z-1)$ -dimensional integral corresponding (Taflanidis and Beck 2006) to integration of a Gaussian probability density function over  $\Delta_i$  and can be efficiently

performed even for larger  $n_z$  values with all required statistics easily obtained from the output covariance matrix of Eq. (6).

### 3.4. Optimization consideration

Calculation of the out-crossing rate facilitates then the reliability-based design given by Eq. (14) which corresponds to a nonlinear, non-convex optimization problem which can be approached by any appropriate algorithm. Further details about this optimization are provided in (Taflanidis and Scruggs 2010).

## 4. DESIGN EXAMPLE AND DISCUSSION

The design approach is illustrated by considering a 10-storey building frame equipped with a single TMDI. The lumped mass per story is 900ton whereas the stiffness has a gradual decrease along height; it is 782.22MN/m for the bottom four stories, 626.10MN/m for the three intermediate ones and 469.57MN/m for the top three stories. Modal damping equal to 3% is considered. The natural periods the structure along with the participation factors in parenthesis are 1.5s (81.7%), 0.55s (11.8%), 0.33s (3.7%). The stationary seismic excitation  $\ddot{x}_g$  is described by a high-pass filtered Kanai-Tajimi power spectrum (Clough and Penzien 1993)

$$S_g(\omega) = s_o \cdot \frac{\omega_g^4 + 4\zeta_g^2 \omega_g^2 \omega^2}{(\omega_g^2 - \omega^2)^2 + 4\zeta_g^2 \omega_g^2 \omega^2} \frac{\omega^4}{(\omega_f^2 - \omega^2)^2 + 4\zeta_f^2 \omega_f^2 \omega^2}. \quad (20)$$

In the above equation the Kanai-Tajimi parameters  $\omega_g$  and  $\zeta_g$  represent the stiffness/frequency and damping properties, respectively, of the supporting ground modeled by a linear damped SDOF oscillator driven by white noise. Further, the parameters  $\omega_f$  and  $\zeta_f$  control the cut-off frequency and the "steepness" of a high-pass filter used to suppress the low frequency content allowed by the Kanai-Tajimi filter. Lastly,  $s_o$  is chosen to achieve a desired pre-specified value for the root mean square acceleration  $a_{RMS}$  of the considered seismic input. For the purposes of this study, the adopted values are  $\omega_g=3\pi$ ,  $\zeta_g=0.4$ ,  $\omega_f=\pi/2$ ,  $\zeta_f=0.8$ ,  $a_{RMS}=0.09g$ .

The vector of structural performance variables  $\mathbf{z}(t)$  includes inter-storey drifts and absolute accelerations for all 10 floors of the structure plus the TMD mass displacement (stroke). The assumed thresholds are chosen as 5cm for interstorey drifts, 1.0g for floor accelerations, and 1m for the stroke. For the uncontrolled structure (without the TMDI) the out crossing rates are  $2.82 \cdot 10^{-2}$  and  $1.19 \cdot 10^{-2}$  when considering only the drifts or accelerations respectively, whereas the out crossing rate for the entire output vector (drifts and accelerations) is  $3.16 \cdot 10^{-2}$ . The comparison between these out-crossing rates demonstrate the strong (but not complete) correlation even between the drift and acceleration responses; total out-crossing rate is greater than the larger of the two but smaller than their sum. Additional correlation does exist between output at different floors.

The assumed vector of dimensionless TMDI design variables is  $\boldsymbol{\varphi} = [\zeta_d f_d \beta]^T$  and includes the damping, frequency and inertance ratios, defined in Eq. (4). The mass ratio  $\mu$  is treated as a fixed pre-specified parameter and a parametric investigation is undertaken for different values of  $\mu$  ranging from 0.1% to 5%. These correspond to additional mass for the  $i_d$  floor (floor where the TMD is attached to) ranging from 1% to 50% of the floor mass. Furthermore, a set of 12 different TMDI topologies are assessed defined by  $i_d$  and  $i_b$  floor pairs (i.e., floor numbers where the TMD and the inerter are attached, respectively) as listed in the first two columns of Table 1. As an example, Figure 2 depicts the case where  $i_d=10$  and  $i_b=9$ , that is the first topology considered in Table 1. Note that, although practical architectural considerations suggest that the inerter would link the  $m_d$  mass to the floor immediately above or below the  $i_d$  floor, cases in which  $|i_d-i_b|=2$  are also examined.

Due to space limitations, attention is herein focused on the optimal TMDI performance in terms of out-crossing rate estimated by Eq. (15) and in terms of the optimal inertance ratio  $\beta$  for which results are reported in Table 1. This choice is justified by the fact that optimal values for the above two quantities are herein derived for the

first time in the literature. However, it is noted in passing that trends for optimal frequency ratio  $f_d$  and damping ratio  $\zeta_d$  parameters not shown here follow, in general, the ones discussed in Marian and Giaralis (2014).

In view of the numerical data in Table 1 pertaining to various TMDI topologies several observations can be made. For one, a definite optimum inertance ratio  $\beta$  is obtained in all cases from the optimization algorithm whose value depends significantly on the mass ratio  $\mu$ . Above a certain critical mass ratio value, the classical TMD (no inerter included) achieves better performance. In other words, the inclusion of the inerter device is more beneficial for relatively small attached masses, an observation previously reported in the literature in terms of top floor displacement variance minimization (Marian and Giaralis 2014). Herein, it is also found that this critical mass ratio value is strongly dependent on the TMDI topology. Examining the structural performance, it is observed that the incorporation of the inerter leads to enhanced vibration suppression compared to the classical TMD. Slightly better performance is achieved for  $i_d > i_b$  compared to the  $i_d < i_b$  (i.e., the attached mass is linked to a lower rather than an upper floor via the inerter) and significantly better performance is achieved for  $|i_d-i_b|=2$  compared to the practically more feasible  $|i_d-i_b|=1$  cases. Further, for the TMDI cases (non-zero inertance) an increase of the mass ratio does not impact the performance significantly. However, an almost linear positive relationship exists between performance and mass ratio for the TMD cases. Interestingly, in some TMDI cases with  $|i_d-i_b|=2$  and  $i_d < i_b$  smaller mass ratio lead to better performance. Overall, placement of the TMDI at lower floors provides greater efficiency, while for the TMD cases higher floor placement seems to be more beneficial. Lastly, it is generally found that the improvement of performance due to the inclusion of the TMDI is remarkable with reduction of out-crossing rates close to order of magnitudes for some cases even for mass ratios as low as 0.1% of the total mass of the structure.

Table 1: Optimal out-crossing rate  $\nu_z^+(\varphi^*) \cdot 100$  and optimal inerter ratio  $\beta$  % (in parenthesis) for different TMDI topologies. The cases for which an optimal value of  $\beta=0$  is obtained are denoted by TMD

TMDI topology		mass ratio $\mu_d$									
$i_d$	$i_b$	0.1%	0.3%	0.5%	0.75%	1%	1.5%	2%	3%	4%	5%
10	9	1.507 (217.7)	1.497 (210.9)	1.487 (204.7)	1.161 (TMD)	0.795 (TMD)	0.381 (TMD)	0.194 (TMD)	0.064 (TMD)	0.028 (TMD)	0.014 (TMD)
10	8	0.348 (122.2)	0.342 (120.1)	0.335 (119.7)	0.327 (114.2)	0.319 (110.1)	0.302 (104.6)				
9	10	1.526 (224.7)	1.554 (230.8)	1.581 (238.34)	1.249 (TMD)	0.881 (TMD)	0.448 (TMD)	0.244 (TMD)	0.093 (TMD)	0.047 (TMD)	0.027 (TMD)
9	8	0.626 (234.7)	0.625 (228.9)	0.623 (223.3)	0.620 (216.4)	0.616 (209.8)					
9	7	0.071 (139.6)	0.071 (136.8)	0.071 (134.7)	0.070 (133.2)	0.070 (129.5)	0.069 (125.9)	0.068 (120.8)	0.066 (111.5)		
8	9	0.634 (240.63)	0.648 (251.0)	0.662 (260.3)	0.677 (341.9)	0.691 (345.8)	0.565 (TMD)	0.331 (TMD)	0.145 (TMD)	0.083 (TMD)	0.057 (TMD)
8	10	0.355 (126.5)	0.365 (133.2)	0.373 (151.2)	0.382 (152.4)	0.392 (153.3)	0.411 (156.3)	0.331 (TMD)			
8	7	0.276 (315.85)	0.279 (309.7)	0.281 (303.5)	0.284 (296.4)	0.287 (296.5)	0.292 (277.7)	0.297 (266.5)			
8	6	0.024 (180.27)	0.025 (176.6)	0.025 (173.2)	0.025 (169.9)	0.026 (167.1)	0.027 (161.9)	0.027 (157.4)	0.028 (148.5)	0.029 (139.6)	0.030 (129.6)
7	8	0.278 (326.6)	0.285 (341.9)	0.291 (413.9)	0.299 (416.7)	0.306 (420.1)	0.322 (424.9)	0.338 (429.7)	0.204 (TMD)	0.117 (TMD)	0.079 (TMD)
7	9	0.072 (143.7)	0.074 (151.3)	0.076 (171.8)	0.079 (172.5)	0.082 (174.6)	0.087 (176.8)	0.093 (179.4)	0.105 (184.1)	0.118 (188.7)	
7	6	0.135 (418.5)	0.137 (413.9)	0.139 (410.4)	0.141 (404.3)	0.144 (403.6)	0.148 (394.0)	0.153 (387.2)	0.163 (376.6)	0.117 (TMD)	

To shed more light in the above comparisons, Figure 4 plots the transfer function of the absolute top floor acceleration for the uncontrolled (primary) structure, for three different optimal TMDI cases for  $\mu=1\%$  and for an optimal TMD case for  $\mu=5\%$ . Evidently, TMDI leads to a fundamentally different behavior than the classical TMD, impacting a greater range of natural frequencies beyond the fundamental one. Placement of the inerter two floors apart provides an even more broad-band influence. This demonstrates that a proper design for a TMDI needs to account for a wide frequency response range and should not target only the fundamental mode as in the case of reliability-based design of the classical TMD (Marano et al. 2007). The proposed state-space analysis approach and, especially, the consideration of the correlation between failure modes facilitate seamlessly this goal.

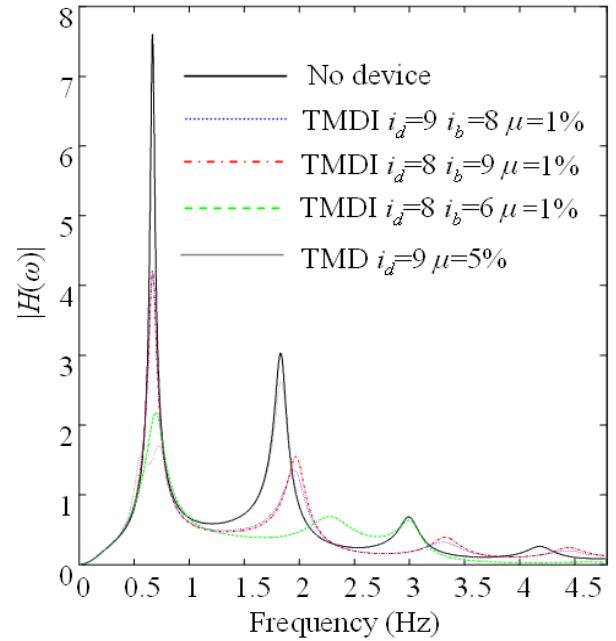


Figure 4: Absolute value of transfer function for the top floor acceleration for 4 different topologies.

## 5. CONCLUDING REMARKS

A first-passage reliability based approach was considered for the optimum design of the recently proposed tuned mass-damper-inerter (TMDI) system to control the dynamic response of linear building frames subject to stationary seismic excitations. Different failure modes were examined for defining acceptable performance, extending to inter-storey drifts and floor acceleration responses for the primary structure as well as displacement responses of the attached mass. The design variables included the inertance (mass amplification property) of the inerter as well as the TMDI linear spring and damping constants. The illustrative example demonstrated the enhanced performance of the TMDI over the classical TMD especially for relatively small additional attached mass. Future work will include treating the mass ratio as a design parameter as well as the consideration of TMDI topology optimization. Further, the robustness of the TMDI to uncertain seismic excitation properties and their non-stationary nature, including ground motions with forward directivity pulses, and to uncertain primary structure properties will also be assessed.

## 6. REFERENCES

Clough, R. W., and Penzien, J. (1993). *Dynamics of structures*, McGraw-Hill Inc., New York, N.Y.

Hoang, N., Fujino, Y., and Warnitchai, P. (2008). "Optimal tuned mass damper for seismic applications and practical design formulas," *Eng Struct*, 30, 707-715.

Lutes, L. D., and Sarkani, S. (1997). *Stochastic analysis of structural and mechanical vibrations*, Prentice Hall, Upper Saddle River, NJ.

Marano, G. C., Greco, R., Trentadue, F., and Chiaia, B. (2007). "Constrained reliability-based optimization of linear tuned mass dampers for seismic control." *Int J Solids Struct*, 44(22-23), 7370-7388.

Marian, L., and Giaralis, A. (2013), "Optimal design of inerter devices combined with TMDs for vibration control of buildings exposed to stochastic seismic excitations," *11<sup>th</sup> International*

*Conference on Structural Safety and Reliability* (June 16-20, 2013, NY), paper #137, 1025-1032.

Marian, L., and Giaralis, A. (2014). "Optimal design of a novel tuned mass-damper-inerter (TMDI) passive vibration control configuration for stochastically support-excited structural systems." *Prob Eng Mech*, 38, 156-164.

Marian, L., and Giaralis, A. (2015). "Vibration suppression, weight reduction, and energy harvesting for harmonically excited structures using the tuned mass-damper-inerter (TMDI)," *Struct Cont Health Mon*, submitted.

Moutinho, C. (2012). "An alternative methodology for designing tuned mass dampers to reduce seismic vibrations in building structures," *Earth End Struct D*, 41, 2059-2073.

Papageorgiou, C., and Smith, M.C. (2005). "Laboratory experimental testing of inerters," *IEEE Conference on Decision and Control*, 44, 3351-3356.

Rana, R., and Soong, T.T. (1998). "Parametric study and simplified design of tuned mass dampers," *Eng Struct*, 20(3), 193-204.

Rice, S. O. (1944, 1945). "Mathematical analysis of random noise." *Bell System Technical Journal*, 23 and 24.

Smith, M.C. (2002). "Synthesis of mechanical networks: The Inerter," *IEEE Transactions in Automatic Control*, 47(10), 1648-1662.

Swift, S.J., Smith, M.C., Glover, A.R., Papageorgiou, C, Gartner, B., and Houghton, N.E. (2013). "Design and modelling of a fluid inerter," *Int J Control*, 86 (11), 2035-2051.

Taflanidis, A. A., and Scruggs, J. T. (2010). "Performance measures and optimal design of linear structural systems under stochastic stationary excitation." *Struct Saf*, 32(5), 305-315.

Takewaki, I., Murakami, S., Yoshitomi, S., and Tsuji, M. (2012). "Fundamental mechanism of earthquake response reduction in building structures with inertial dampers," *Structural Control and Health Monitoring*, 19, 590-608.

Tigli, O.F. (2012). "Optimum vibration absorber (tuned mass damper) design for linear damped systems subjected to random loads," *J Sound Vib*, 331, 3035-3049.

Wang, F.C., Hong, M.F., and Lin, T.C. (2011). "Designing and testing a hydraulic inerter," *J Mech Eng Sci*, 225(1), 66-72.